Velocity dependence of nano-abrasive wear of amorphous polymers obtained using a spiral scan pattern

Reginald H. Rice, Enrico Gnecco, Reinhold Wannemacher, and Robert Szoszkiewicz

Published Version Information

Citation: Rice, R. H., Gnecco, E., Wannemacher, R., & Szoszkiewicz, R. (2013). Velocity dependence of nano-abrasive wear of amorphous polymers obtained using a spiral scan pattern. Polymer, 54(14), 3620-3623.

Digital Object Identifier (DOI): doi:10.1016/j.polymer.2013.05.015

Publisher's Link: http://www.sciencedirect.com/science/article/pii/S0032386113004461

Velocity dependence of nano-abrasive wear of amorphous polymers obtained using a spiral scan pattern

Reginald H. Rice[(1)], Enrico Gnecco[(2)], Reinhold Wannemacher[(2)], and Robert Szoszkiewicz[(1)]

(1) Department of Physics, Kansas State University, Manhattan, Kansas 66506, USA

(2) Instituto Madrileño de Estudios Avanzados en Nanociencia (IMDEA Nanociencia), Campus Universitario de Cantoblanco, Calle Faraday 9, 28049, Madrid, Spain

We demonstrate how the wear response of a polymer surface can be efficiently characterized by atomic force microscopy (AFM) using a spiral scan with a thermal tip. If the spiral is scanned at constant angular speed in the vicinity of the glass transition of the polymer, the corrugation of the modified surface is found to decay exponentially with the linear velocity v. This is attested by profiles on poly(methyl methacrylate), PMMA, and polystyrene, PS, surfaces obtained at AFM tip-surface temperatures up to 115 °C. We show that quantitative information for modeling polymer wear on the nanoscale can be obtained from this kind of measurements.

Corresponding author: Robert Szoszkiewicz, PHONE: 785-532-0855, FAX: 785-532-6806, EMAIL: szosz@ksu.edu

Graphical Abstract

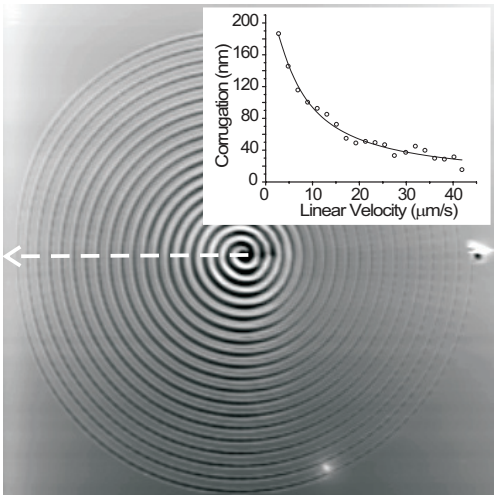

Introduction

One of the most interesting, but less exploited features of AFM is its capability of locally modifying the morphology of a surface and tracking its variations before, after, and during the modification process. For instance, periodic ripple patterns can be formed on polymers [1, 2], metals [3], ionic crystals [3] and semiconductors [4] if the probing tip of an AFM repeatedly scans back and forth on these surfaces with a normal pressure exceeding the yield strength of the material. Polymers can also be patterned with a single scan line when the temperature of the contact region exceeds the glass transition temperature of the sample [5].

In most experimental investigations, the scan path of the probing tip is the same as the one usually adopted for imaging the sample surface, i.e. zigzag or raster scanning on a square area. However, while the scanning pattern does not play an important role for imaging, the situation is very different when the surface is worn out by the tip. In a recent study, we have indeed observed 'traveling' ripples when a circular track is continuously scanned [6]. In that case one can measure the 'group velocity' of the ripples and relate it to the wear rate of the material. In the present Letter we focus on a different shape, i.e. an Archimedean spiral, and take advantage of its geometric properties to study the abrasive response of polymers at temperatures elevated locally at the tip-sample interface. In this way, a single AFM image acquired after scratching the polymer surface can provide important information for a quantitative characterization of the velocity dependence in nano-wear processes with applications

in NEMS, MEMS as well as polymer coatings.

Experimental

The polymers used in this study are PMMA and PS polymers from American Polymer Standards Corporation, with weight average molar mass $M_{w,\mathrm{PS}} = 215.7$ kg mol^{-1} and $M_{w,\mathrm{PMMA}} = 120$ kg mol^{-1}, and polymer polydispersity 1.1. The PMMA film was produced by spin coating 2.5 % wt polymer solution in chloroform on soda lime fine polished glass substrate from Fisher Scientific. The PS film was produced by spin coating 2.5 % wt polymer solution in toluene on same type of glass substrate as the PMMA. In both cases spin coating was done at 500 rpm for 10 s and 2000 rpm for remaining 50 s. HPLC-grade toluene and HPLC-grade chloroform from Sigma-Aldrich were used. Furthermore, the PMMA sample was annealed 15.5 h at 55 °C followed by 1 h at 90 °C and the PS sample was annealed 14 h at 85 °C followed by 2.5 h at 120 °C. The usage of 120 °C (above T_g) was dictated by the observation that after 14 h at 85 °C the samples still showed some local pits, so the temperature was ramped up to make the surface smooth. The resulting PMMA film thickness of 240 ± 60 nm was determined by a scratch test with AFM.

For producing spirals at various tip-sample temperatures we used cantilevers with integrated heaters [7, 8], which were mounted in a di-CP-II AFM system equipped with a module to read their temperature [6, 9]. The tip temperature calibration was based on acquiring indentation profiles on two polymer samples with known softening temperatures [8–10]. The elastic spring constants of thermal levers are typically between 0.6-0.7 N/m and are obtained using the thermal noise method on our other custom-made AFM system [11]. From the SEM images, see Supplementary Materials, the radius of curvature of the tip apex in the transverse direction ($R_x = 120 \pm 10$ nm) is significantly smaller than its longitudinal radius ($R_y = 170 \pm 10$ nm). The AFM topographs of the polymer films with the spirals were recorded in contact mode with Proscan software and SiN_x MLCT-D cantilevers, all from Bruker USA. The cantilevers had a nominal elastic spring constant between 0.04 to 0.07 N/m and nominal curvature radii below 20 nm. Assuming that the radial distance r of the spiral grows linearly with the time t as $r(t) = \alpha t$, and that the angular velocity ω is

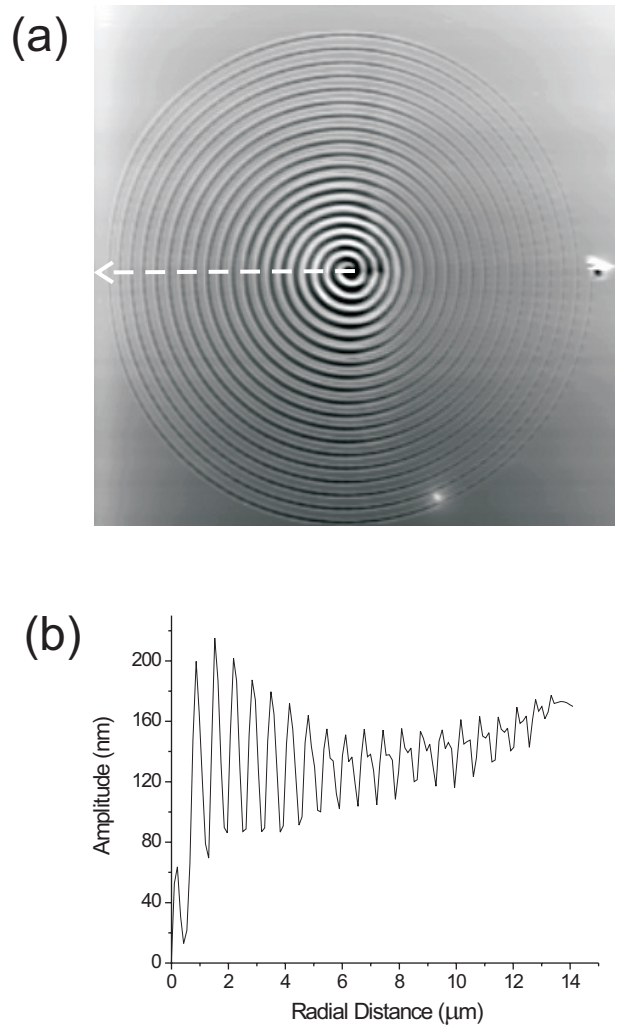

FIG. 1: (a) An Archimedean spiral on PS made with a hot-tip AFM with a normal force $F_N = 10 \pm 3$ nN and an angular velocity $\omega = 3.14$ s^{-1}. This topography rescan (frame size: 28 μm) was obtained with a regular contact mode AFM using MLCT-D lever from Bruker at load of 2 ± 1 nN. (b) A cross section along the dashed lines in (a).

constant, it is easy to see that the linear velocity v of the probing tip grows with r as $v = \sqrt{\alpha^2 + (\omega r)^2}$. This dependence becomes almost linear, and the velocity almost tangential, when $r \gg \alpha/\omega$, which is the case for all spiral windings in our experiment, except the very first one.

Results and Discussion

Fig. 1(a) shows a representative AFM topograph of a spiral generated on the PS sample at 206 °C on the cantilever, which corresponds to 97±12 °C on the tip-sample interface (see Supplementary Information for details on temperature calibration). A cross section profile is shown in Fig. 1(b). We note that in the first windings the material pushed aside of the groove partially overlaps, whereas this is not the case after the eighth revolution of the tip around the spiral center. In any case, the amplitude of the indentation profile dramatically decreases with the scan speed. Intuitively, this can be understood as follows. The longer the tip keeps indenting a given spot on the surface, the more damage is caused, so that the amplitude is expected to decay with v. To explore this assumption we have plotted the corrugation as a function of the scan velocity (Fig. 2).

In a previous AFM analysis on abrasive nanowear of alkali halides [12] we found that the wear rate decreases exponentially with the 'time of residence' spent by the tip at a given location on the surface. A similar assumption was proposed by Mulhearn and Samuels to interpret the abrasion of steel sliding against silicon carbide paper [13]. Since in the present case the time of residence is inversely proportional to the scan velocity, we have thus fitted the data points in Fig. 2 with the following function:

$$h(v) = h_0 \left[1 - \exp\left(-\frac{v_0}{v}\right)\right]. \qquad (1)$$

As shown by the continuous curve in Fig. 2, an excellent agreement is found when $h_0 = 209 \pm 10$ nm and $v_0 = 6.0 \pm 0.4$ μm/s. In equation (1) the parameter h_0 corresponds to the indentation depth of the sample at a given load, when the tip is not driven along the surface, whereas the parameter v_0 quantifies how fast the wear damage decays with the linear speed.

This analysis is extended to other spirals obtained in the PMMA and PS samples at different conditions. In particular, we have explored the range of temperatures around the glass transition, which occurs at 95 ± 5 °C and 105 ± 5 °C for the PS and PMMA samples respectively. The limit value h_0 was always in the range of 100 nm, i.e. comparable to the obtained corrugations, whereas the 'decay velocity' v_0 remained in the order of 10 μm/s in the series of measurements that we performed. However, the values of both quantities exhibit significant scattering. This is not

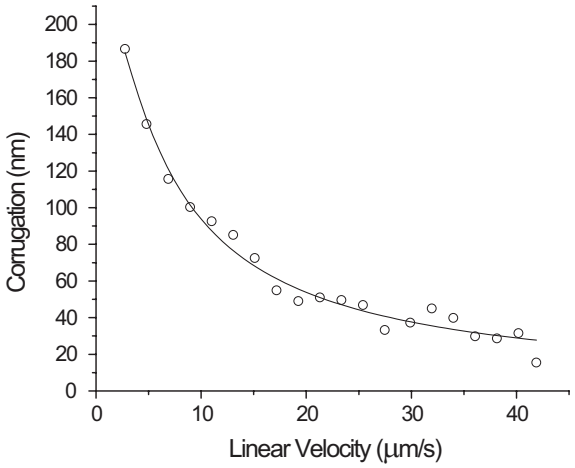

FIG. 2: Corrugation profile obtained from Fig. 1(b) by subtracting the maximum height of the material pushed aside from the indentation depth of each groove along the profile. Corrugation profile is fitted by the equation (1) with $h_0 = 209 \pm 10$ nm and $v_0 = 6.0 \pm 0.4$ μm/s.

surprising, since the roughening rate of polymers on the nanoscale has been reported to peak up and scatter in the region of T_g [14]. Even more scattered are the values for the 'decay velocity' v_0, which was found to vary between 0.6 and 7 μm/s in the series of measurements that we performed.

Two extreme cases, corresponding to $v_0 = 5 \pm 1$ μm/s and 0.6 ± 0.2 μm/s respectively, are showed in Fig. 3(a) and (b). The spiral in Fig. 3(a) was obtained on PMMA at 97 ± 12 °C. In this case the corrugation did not decrease significantly after the first windings, as if the material opposed almost no resistance to ploughing. This is not the case for the spiral in Fig. 3(b), the amplitude of which quickly decayed after only two revolutions. However, this spiral was produced at lower temperature of 89 ± 12 °C at the tip-sample interface, which is below the glass transition of PMMA. We should also note that the indentation patterns along each winding are not varying uniformly, but undulate, which is presumably related to the elongated shape of the tip apex. On the other side, since the different spring constants of the cantilever in the x and y direction do not influence the contact stiffness responsible for friction (and wear) on the sample surface [15], the torsional and bending deformations of the cantilever seem not to have a major influence on the spiral patterning.

In order to interpret our results we first notice that stationary heat flow below

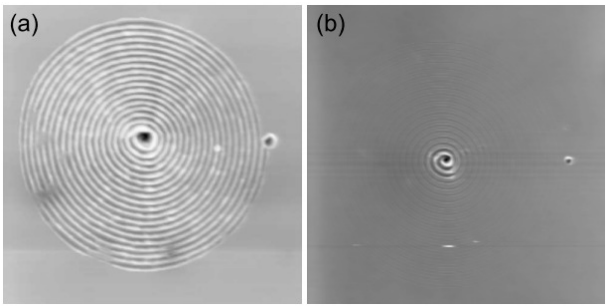

FIG. 3: As the glass transition temperature is approached, the response of a polymer surface to nano-ploughing can be quite variable. This is shown in the case of two spirals made on an initially flat PMMA surface (a) at 97 ± 12°C and (b) at 89 ± 12°C. Frame sizes: 15 μm.

the heated tip is reached within a very short time of less than 1 μs. This is proven by numeric solutions of the heat equation at different indentation depths, which are detailed in the Supplementary Materials. For comparison, the residence time τ of the heated tip while writing a spiral is in the order of 1-100 ms, see below. Thus, we can assume that, when the tip apex is heated above T_g, a sample region beneath enters a heavily viscous state almost instantaneously.

Approximating the tip by a sphere of radius R, the observed corrugations h correspond to contact radii $a = (h(2R - h))^{1/2}$, which are significantly larger than the values predicted by the elasto-plastic contact mechanics, $a = 3.2(RF/Y)^{1/3}$ [16]. For example, with a tip radius $R = 150$ nm, a reduced Young modulus for PS $Y = 1$ GPa [17], and a normal force $F = 10$ nN, we obtain $a \simeq 40$ nm, whereas indentation depths of up to about 100 nm, corresponding to contact radii of about 140 nm, are observed in Figure 1. This confirms that finite viscosity of the polymer must be taken into account in order to explain the observed corrugations at $T \geq T_g$. The corrugations are produced during the residence time τ. Within this time a polymer volume V equal to the volume of the tip beneath the polymer, is squeezed out by the tip. Kobayashi et al. [18] have studied the viscosities of PMMA as well as PS around the glass transition temperature. They reported that polymer viscosity varies by at least one order of magnitude when the temperature deviates from T_g by only about 5 %, i.e. by about 20 K in our case. Our thermal simulations, see Supplementary Materials, indicate that only a thin polymer layer of width δ of about 20 nm around

the tip corresponds to that temperature range and is therefore sufficiently softened to contribute to the viscous mass transfer. Once a viscous material is released out of the wear groove and looses contact with the tip, it quickly solidifies, giving rise to the elevations aside the wear scar. The process ends when the pulling force exerted by the cantilever reaches a critical value and the tip suddenly jumps in a stick-slip fashion [19].

Interestingly, using our data, we can calculate and comment on the viscous matter flow. From Figure 1, near the center of the spiral at $r \simeq 2$ μm, the values of $h \simeq$ 100 nm, $a \simeq 140$ nm, $v_{tip} \simeq 6$ μ/s, and $\tau \simeq 50$ ms. Here, r is the distance measured from the center of a spiral and the value of τ was calculated by dividing twice the contact radius a by the tip velocity v_{tip}. At the outer limit of the spiral for $r \simeq 13$ μm, $h \simeq 5$ nm, $a \simeq 40$ nm, $v_{tip} \simeq 40$ μm/s, and $\tau \simeq 2$ ms. To calculate the viscous flow in such two cases, we suppose that the material of volume V is squeezed out from underneath the tip within the residence time τ through a ring of width δ on the surface adjacent to the tip and with a radius determined by the instantaneous contact radius during the indentation, which assumes values between 0 and a. For simplicity, let us use the flow velocity, v_{flow}, for a mean ring diameter of $(1/2)a$. The value of $v_{flow} = V/(A\tau)$, where A is an area of a ring $A = \pi(a/2 + \delta)^2 - \pi(a/2)^2 \simeq \pi a\delta$. Approximating the tip as a sphere of radius R, the value of $V = \pi h^2(3R - h)/3$ is calculated. Using $\delta = 20$ nm the value of v_{flow} decreases from ~ 9 μm/s to ~ 2 μm/s from the center of a spiral to its outer limit, respectively. The maximum shear stress within this flow occurs at the walls of the viscous layer under the tip and is estimated by assuming laminar flow with a shear rate $\dot{\epsilon} = 6v_{flow}/\delta \simeq 10^3$ s^{-1}. Using the Newtonian viscosity of PMMA at $T \simeq T_g$ determined by Kobayashi et al. [18], $\mu \simeq 10^8$ Pa $\cdot$ s, the resulting shear stress σ due to viscous flow is $\sigma = \mu\dot{\epsilon} \simeq 10^{11}$ N$\cdot$ m^{-2}. The applied compressive stress, on the other hand, proportional to and of the same order of magnitude as the shear stress, is about $F/(\pi a^2)$. With the contact radii estimated above, between 40 nm and 140 nm, values of the compressive stress of 10^5 and 10^6 N$\cdot$ m^{-2} are obtained, i.e. 5-6 orders of magnitude smaller than the value derived from our experiment and the thermal simulation. In order to explain this discrepancy we have to take into account that the polymer viscosity becomes highly non-Newtonian at strain rates of 10^4 s^{-1}. This may result in considerable shear

thinning [20]. To the best of our knowledge measurements of the non-Newtonian viscosity and shear thinning of polymers at temperatures $T \simeq T_g$ and high strain rates have not been undertaken so far. It should be noted that a similar discrepancy was observed in the IBM Millipede project for data storage in polymer materials by heated tips [21]. A significant contribution coming from plastic deformation of the non-melted part of the polymer should also be taken into account in a more accurate modeling of the wear process.

Finally, we have also observed the formation of ripples inside all spiral tracks, resulting from the stick-slip mechanism mentioned above [19]. An example is given in Fig. 4, showing the surface profile in the bottom of a spiral. The ripples are radially aligned, which means that their periodicity is proportional to the radial distance r as well as to the scan velocity v. The ripple wavelengths are comparable to our earlier results of ripples produced in circular scanning in the vicinity of the glass transition temperature on PMMA [6] at corresponding velocities. Although the ripples are seen along the whole spiral, they are more pronounced in two quadrants. This is related to the asymmetry of the indentation patterns previously discussed and asymmetric tip profile of a thermal cantilever. Namely, more elongated ripples appear along longitudinal scanning direction, which correlates with a larger longitudinal than transverse curvature radius of the thermal tip.

Conclusions

In conclusion, we have introduced a simple method to characterize the velocity dependence of the wear rate on polymer surfaces. The surface is first scanned by contact AFM adopting a spiral pattern, the damaged area is then rescanned using a 'standard' raster pattern and the surface corrugation is finally extracted using azimuthal profiles along the spiral and fitted with an exponential decay law. This method can be extended to other materials, provided that they are brittle enough to be damaged within a single scan. We have also showed that quantitative information for modeling abrasive wear on the nanoscale can be obtained from this kind of measurements.

The Spanish Ministry of Science and Innovation (Project No. MAT3011-26312) (EG) are gratefully acknowledged for financial support. We also thank Prof. William

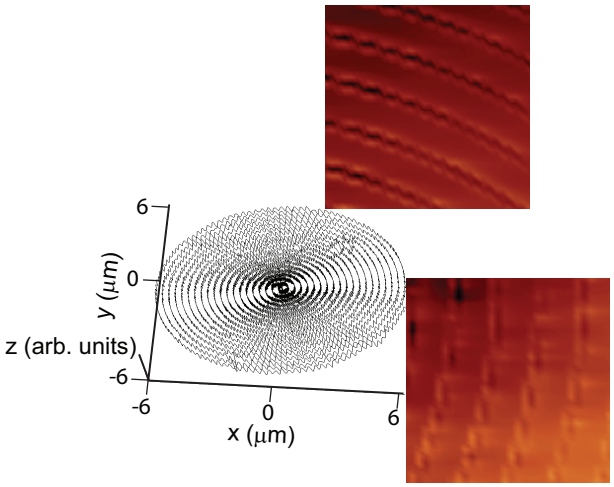

FIG. 4: Occurrence of surface ripples along a spiral groove. The undulation is enhanced in two quadrants of the xy plane. INSET: Two 1.7 μm by 1.7 μm AFM topography rescans showing surface ripples along horizontal and vertical portions of the spiral, respectively.

P. King for his invaluable assistance with thermal AFM cantilevers.

---

[1] O. M. Leung and M. C. Goh, Science **255**, 64 (1992).

[2] Z. Elkaakour, J. P. Aime, T. Bouhacina, C. Odin, and T. Masuda, Phys. Rev. Lett. **73**, 3231 (1994).

[3] A. Socoliuc, E. Gnecco, R. Bennewitz, and E. Meyer, Phys. Rev. B **68**, 115416 (2003).

[4] B. Such, F. Krok, and M. Szymonski, Appl. Surf. Sci. **254**, 5431 (2008).

[5] R. H. Schmidt, G. Haugstad, W. L. Gladfelter, Langmuir **15**, 317 (1999).

[6] E. Gnecco, E. Riedo, W. P. King, S. R. Marder, and R. Szoszkiewicz, Phys. Rev. B **79**, 235421 (2009).

[7] P. Vettiger, M. Despont, U. Drechsler, U. Durig, W. Haberle, M. I. Lutwyche, H. E. Rothuizen, R. Stutz, R. Widmer, and G. K. Binnig, IBM J. Res. Dev. **44**, 323 (2000).

[8] J. Lee, T. Beechem, T. L. Wright, B. A. Nelson, S. Graham, W. P. King, W. P., J. Microel. Sys. **15**, 1644 (2006).

[9] R. Szoszkiewicz, T. Okada, S. C. Jones, T. D. Li, W. P. King, S. R. Marder, and E. Riedo, Nano Lett. **7**, 1064 (2007).

[10] B. A. Nelson and W. P. King, Sens. Act. A: Phys. **140**, 51 (2007).

[11] A. Dey and R. Szoszkiewicz, Nanotech. **23**, 175101 (2012).

[12] E. Gnecco, R. Bennewitz, and E. Meyer, Phys. Rev. Lett. **88**, 215501 (2002).

[13] O. Mulhearn and L. E. Samuels, Wear **5**, 478498 (1962).

[14] R. H. Schmidt, G. Haugstad, W. L. Gladfelter, Langmuir **19**, 10390 (2003).

[15] P. Steiner, R. Roth, E. Gnecco, A. Baratoff, S. Maier, T. Glatzel, and E. Meyer, Phys. Rev. B **79**, 045414 (2009).

[16] Springer Handbook of Nanotechnology, edited by B. Bhushan, Springer-Verlag, Heidelberg (2004).

[17] J. Richeton, G. Shlatter, K. S. Vecchio, Y. Remond, and S. Ahzi, Polymer **46** 8194-8201 (2005).

[18] H. Kobayashi, H. Takahashi, and Y. Hiki, J. Non-Cryst. Sol. **209**, 32-40 (2001).

[19] R. H. Rice, P. Mokarian-Tabari, W. P. King, and R. Szoszkiewicz, Langmuir **28**, 13503-11 (2012).

[20] D. W. van Krevelen, Properties of polymers, pp. 60-3, Elsevier, Amsterdam (1990).

[21] P. Vettiger, G. Cross, M. Despont, U. Drechsler, U. Durig, B. Gotsmann, W. Haberle, M. A. Lantz, H. E. Rothuizen, R. Stutz, and G. K. Binnig, IEEE Trans. Nanotechnology **1**, 39 (2002).